RSC Advances

RSC Advances

www.rsc.org/advances

ROYAL SOCIETY OF CHEMISTRY

www.rsc.org/advances

TOC

We report the reduction of 4-nitrophenol catalyzed by silver nanoparticles supported on polymer micelles and vesicles which can significantly improve the stability, dispersibility and catalytic activity of silver nanoparticles even at one ppm.
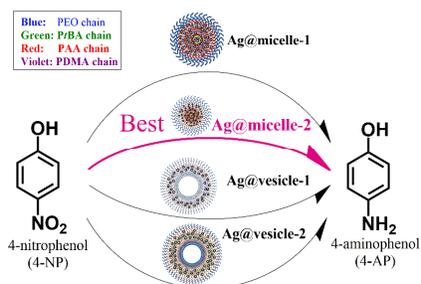
ARTICLE TYPE

Reduction of 4-nitrophenol catalyzed by silver nanoparticles supported on polymer micelles and vesicles

Qingrui Geng and Jianzhong Du*

We report the reduction of 4-nitrophenol catalyzed by silver nanoparticles supported on polymer micelles and vesicles which can significantly improve the stability, dispersibility and catalytic activity of silver nanoparticles even at one ppm.

10 Recently, noble metallic nanoparticles have attracted much interest due to their wide applications in sensing,[1] photochemistry,[2] medicine[3] and catalysis.[4] Among them, silver nanoparticles are particularly attractive because of their good relative abundance, low cost and wide applications.[5] They can be 15 used as effective catalysts with high reactivity and excellent selectivity. However, they are usually easy to aggregate together to minimize their surface area, leading to attenuation of their catalyst efficiency.[6] In order to avoid agglomeration, various supports had been developed to immobilize silver nanoparticles, 20 including alginate gel,[7] silica,[8] carbon nanofibers,[6] titania,[9] and dendrimers, etc.[10] On the other hand, polymer micelles and vesicles have great potential in gene and drug delivery,[11] antibacterial agents,[12, 13] templates for biomineralization,[14] etc. Furthermore, O'Reilly *et al.* prepared *L*-proline-containing 25 polymer micelles to catalyze the direct asymmetric aldol reaction in water.[15] Chen and co-workers showed that silver-decorated polydiacetylene vesicles had good nonlinear optical properties.[16]

The reduction of 4-nitrophenol (4-NP) to 4-aminophenol (4-AP) has been widely used to manufacture 4-AP as photographic 30 developers, corrosion inhibitors, anticorrosion-lubricants, and hair-dyeing agents.[17] Various metal nanoparticles such as Ag, Au, Cu, Pt, and Pd in different substrates such as dendrimers, polyelectrolytes, biological cells, *etc.* have been used as the catalyst.[10, 18] However, one fatal drawback is that the addition of 35 NaBH$_4$ will destroy their colloid stability, causing catastrophic aggregation and deactivation of catalytic performance.[19] Also, traditional solid silver catalysts need to be stirred with reactants.[20]

Very recently we reported that polymeric supports such as micelles and vesicles can significantly enhance the dispersibility 40 and stability of silver nanoparticles, leading to excellent antibacterial activities.[21-23] We suppose that those polymeric supports may also significantly improve the stability and catalytic activity of silver nanoparticles without stirring due to the excellent dispersibility of polymer vesicles and micelles in water.

45 In this paper we evaluate the catalytic activities of four silver nanoparticles supported by polymer micelles and vesicles (Table 1), including three reported silver nanoparticles which showed excellent antibacterial activities,[22, 23] and a newly designed

polymer vesicle-supported catalyst, Ag@PEO$_{43}$-*b*-P(*t*BA$_{56}$-*stat*-50 AA$_9$) vesicles (Ag@vesicle-2 in Scheme 1, Table 1, Fig. S1 and S2†).

Scheme 1 Reduction of 4-nitrophenol to 4-aminophenol catalyzed by silver nanoparticles supported on polymer micelles and vesicles (Table 1).
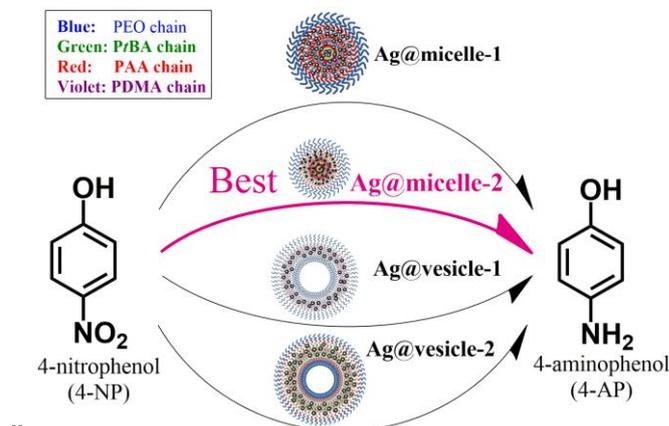

55

Table 1 Silver nanoparticles supported on different polymer micelles and vesicles and their catalytic activities at 25 °C.

Catalyst	Polymer Composition^a	d_{TEM} (nm)^b	TOF (h^{-1})^c
Ag@micelle-1	PEO$_{43}$-*b*-P(DMA$_{27}$-*stat*-*t*BA$_{32}$-*stat*-AA$_{49}$)	1.0 ±2.8	2.09
Ag@micelle-2	PEO$_{43}$-*b*-P(*t*BA$_{15}$-*stat*-AA$_{50}$)	5.6 ±0.8	48.7
Ag@vesicle-1	PEO$_{43}$-*b*-P(DMA$_{31}$-*stat*-*t*BA$_{81}$)	1.9 ±0.4	-
Ag@vesicle-2	PEO$_{43}$-P(*t*BA$_{56}$-*stat*-AA$_9$)	3.1 ±1.9	5.71

^{a}PEO, DMA, *t*BA and AA stand for poly(ethylene oxide), 2-(dimethylamino)ethyl methacrylate, *tert*-butyl acrylate and 60 acrylic acid, respectively. ^{b}The diameter of silver nanoparticles measured by TEM. ^{c}Turnover frequency. The TOF of Ag@vesice-1 is extremely low.

The reduction of 4-NP to 4-AP was carried out in a quartz 65 cuvette in the presence of 1.9 mL of as-prepared aqueous silver nanoparticles solution and 10 μL of aqueous 4-NP solution without stirring. Borohydride (NaBH$_4$) was added after well mixing of the catalysts and 4-NP. To study the effect of the catalyst dosage, the concentrations of silver nanoparticles were 70 varied in the range of 1.0-5.0 μg/mL for Ag@micelle-1, Ag@micelle-2, Ag@vesicle-2, and of 14.0-18.5 μg/mL for Ag@vesicle-1. For all the reduction reactions, the temperature was 25 °C and the final concentrations of 4-NP and NaBH$_4$ were

kept at 5.0×10^{-5} mol/L and 6.6×10^{-3} mol/L, respectively.

Although the reaction is a thermodynamically feasible process involving the standard electrode potential (E_0) of -0.76 V (for 4-NP/4-AP) and -1.33 V (for H_3BO_3/BH_4^-) versus NHE, it is still kinetically restricted in the absence of a catalyst (does not occur even in 2 days' time).[7] In the presence of catalyst, reduction of 4-nitrophenol should happen on the surface of silver nanoparticles with surface-hydrogen species given by BH_4^- (according to classical Langmuir–Hinshelwood model).[24] Under alkaline conditions, the decomposition of borohydride is much slower. The reduction of 4-NP can be easily monitored through spectrophotometry (λ_{max} = 400 nm for 4-nitrophenolate anion). A typical evolution of UV-vis spectra with time in the presence of Ag@micelle-1 (1.0 µg/mL) was shown in Fig. S3†. Similar changes are also obtained for other catalysts. For example, in the presence of Ag@micelle-1 catalyst, the reduction can be visualized by the disappearance of the peak at 400 nm (4-NP) with the concomitant appearance of a new peak at 290 nm (4-AP). After the completion of reduction, the ultimate solution was bleached from yellow color.

In order to compare the catalytic activity of silver nanoparticles on different supports, the silver concentration was set at 1.0 µg/mL. The conversion of 4-NP to 4-AP is calculated by the following equation:

$$\text{Conversion} = (1 - A_t/A_0) \times 100\%$$

Where A_t stands for the UV absorbance at 400 nm, which is proportional to the concentration of produced 4-NP; A_0 is the initial UV absorbance at 400 nm after addition of $NaBH_4$.

The plots of conversion verses time for four different silver nanoparticles are given in Fig. 1, suggesting that Ag@micelle-2 has the best catalytic activity, followed by Ag@vesicle-2, Ag@micelle-1 and Ag@vesicle-1. Their turnover efficiencies (TOFs) indicated their different catalytic activities (Table 1). The polymer composition and morphology of polymer supports play important roles in the growth of silver nanoparticles, which determine their size and surface area, finally affect their catalytic activities.[25, 26]

Ag@micelle-2 catalyst was made from a role switching method.[22] Ag^+ ions were initially evenly absorbed and stabilized in a PEO_{43}-b-P(tBA$_{15}$-$stat$-AA$_{50}$) vesicle template by the electrostatic interaction with negatively charged PAA chains in the vesicle membrane. After addition of the reducing agent $NaBH_4$, the vesicles deformed into small micelles.[22] The produced silver nanoparticles were very uniform (5.6 ± 0.8 nm), giving most effective surface area among four catalysts and leading to the best catalyst among four silver nanoparticles.

In contrast, Ag@micelle-1 catalyst was prepared by introduction of $AgNO_3$ in the core of the PEO_{43}-b-P(DMA$_{27}$-$stat$-tBA$_{32}$-$stat$-AA$_{49}$) micelle and subsequent *in situ* reduction by $NaBH_4$.[23] The silver nanoparticles in Ag@micelle-1 were stabilized by both electrostatic interaction with PAA and coupling with DMA segment. The catalyst has less effective surface area than Ag@micelle-2, leading to a slower reaction rate.

The catalytic activity of Ag@vesicle-2 is much less efficient than Ag@micelle-2 although vesicle-2 has a similar polymer structure to micelle-2. The silver nanoparticles in Ag@vesicle-2 catalyst were formed in the membrane of PEO_{43}-P(tBA$_{56}$-$stat$-AA$_9$) vesicles by a similar *in situ* reduction of $AgNO_3$ and then

stabilized by the electrostatic interaction with PAA. Probably it is because the dense vesicle-2 membrane attenuated the diffusion of 4-NP and $NaBH_4$ to the surface of the silver nanoparticles, leading to a less efficient catalytic activity.

For Ag@vesicle-1 catalyst, the silver nanoparticles were formed in the membrane of the PEO_{43}-b-P(DMA$_{31}$-$stat$-tBA$_{81}$) vesicles and stabilized by the coordination bond between Ag and DMA segment (without PAA in other cases). Although the size of a single silver nanoparticle is the smallest, those silver nanoparticles are densely incorporated in the vesicle membrane, leading to much less effective surface area.[23] Therefore, the catalytic activity of Ag@vesicle-1 catalyst is the worst of all.
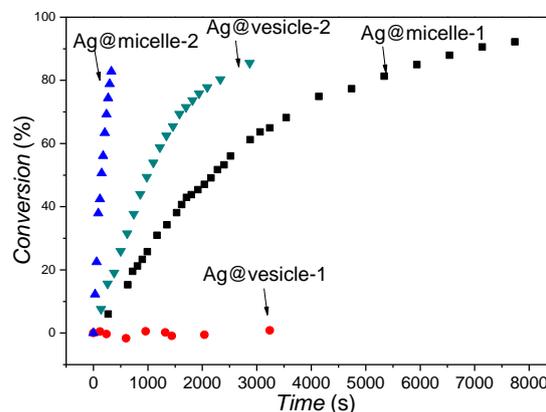

Fig.1 Influence of different polymeric supports on the reduction of 4-nitrophenol (4-NP). Conditions: [4-NP] = 5.0×10^{-5} mol/L, [$NaBH_4$] = 6.6×10^{-3} mol/L, T = 25 ^{o}C.
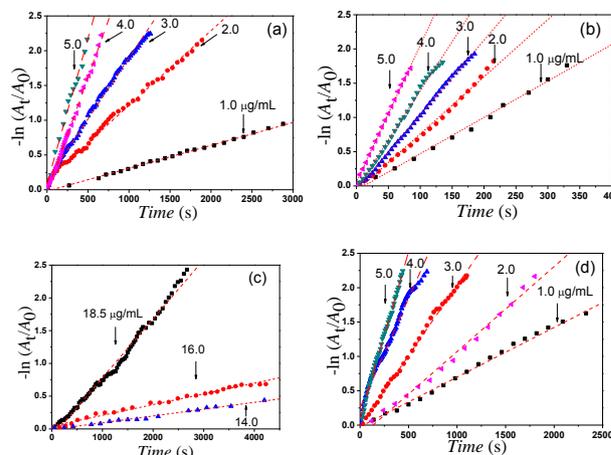

Fig.2 Influence of silver concentration of during the reduction of 4-NP in the presence of (a) Ag@micelle-1; (b) Ag@micelle-2; (c) Ag@vesicle-1; and (d) Ag@vesicle-2. Conditions: [4-NP] = 5.0×10^{-5} M, [$NaBH_4$] = 6.6×10^{-3} M, T = 25 ^{o}C.

The kinetics was studied to investigate the influence of catalyst dosage on the reduction reaction. Because of the large excess of $NaBH_4$ compared to 4-NP, the reduction rate can be considered independent of the borohydride concentration. Therefore, the kinetic data were fitted by Langmuir–Hinshelwood apparent first order kinetics model:[27]

$$r = dC/dt = kKC/(1 + KC)$$

Where r is the reduction rate of the reactant (mg/(L·s)); C is the

concentration of the reactant (mg/L); t is the reaction time; k is the reaction rate constant (mg/(L·s)); K is the adsorption coefficient of the reactant (L/mg). When the initial concentration (C_0) was very low, the above equation could be simplified to an apparent first order model:

$$-\ln(C_t/C_0) = kKt = k_{app}t$$

Where k_{app} is the apparent first-order rate constant (s^{-1}). The reaction progress can be directly read off UV absorbance curves since the ratio of the concentration of 4-NP (C_t) at time t to its initial value C_0 at $t = 0$ is directly given by the ratio of respective absorbance A_t/A_0 by measuring the absorbance at 400 nm from UV spectra. According to the apparent first-order rate equation, when $-\ln(A_t/A_0)$ is proportional to time, the reaction rate corresponds to the slope k_{app} of the curve. In this work, liner relations are found in the plots of $-\ln(A_t/A_0)$ verses time in the reduction of all the four catalysts (Fig. 2a-d). With incremental amount of catalyst, the reaction rate becomes faster accordingly. Ag@micelle-1, Ag@micelle-2 and Ag@vesicle-2 showed much better catalytic performance than Ag@vesicle-1, which only reacted very slowly at the concentration of more than 14.0 μg/mL ($k_{app} = 1.04 \times 10^{-4}\ s^{-1}$).
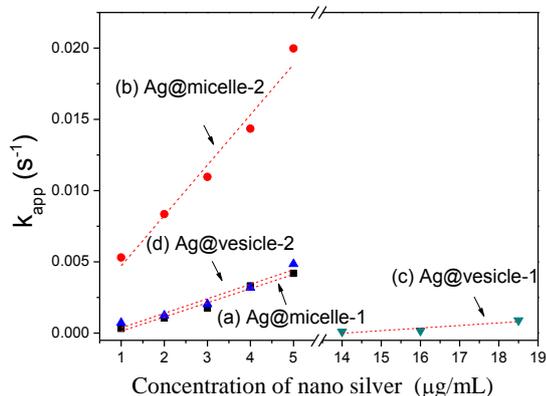

Fig. 3 Plot of rate constant (k_{app}) versus silver concentration for 4-NP reduction by NaBH₄ in the presence of (a)Ag@micelle-1, (b) Ag@micelle-2, (c) Ag@vesicle-1, and (d) Ag@vesicle-2. Conditions: [4-NP] = 5.0×10^{-5} M, [NaBH₄] = 6.6×10^{-3} M, $T = 25\ ^oC$.

The rate constants of silver nanoparticles obtained from Fig. 2 are related to the catalyst dosage (Fig. 3). A linear relation between k_{app} and the concentration of silver nanoparticles is observed.[7] The rate constant increases with the catalyst amount in all cases. The intercept of Ag@micelle-2 is caused by error percentage. At every concentration, Ag@micelle-2 shows a much higher rate constant than others. Ag@vesicle-2 has slightly higher value than Ag@micelle-1 because they are mainly influenced by the coverage of vesicle membrane and DMA coupling, respectively. Ag@vesicle-1 is the worst catalyst due to the influence of both factors.

In summary, silver nanoparticles supported on either polymer micelles or vesicles have showed excellent stability, dispersibility and catalytic activity for reduction of 4-NP. Furthermore, ultrafine silver nanoparticles stabilized by polymer micelles are confirmed to be the best catalyst. Moreover, our strategy provides a new insight for choosing more suitable supports for effective metal nanoparticle catalysts.

Notes and references

School of Materials Science and Engineering, Tongji University, 4800 Caoan Road, Shanghai, 201804, China. E-mail: jzdu@tongji.edu.cn; Fax: +86 (021) 69584723; Tel: +86 (021) 6958 0239

1. J. N. Anker, W. P. Hall, O. Lyandres, N. C. Shah, J. Zhao and R. P. Van Duyne, *Nat. Mater.*, 2008, **7**, 442-453.
2. R. Jin, Y. Charles Cao, E. Hao, G. S. Metraux, G. C. Schatz and C. A. Mirkin, *Nature*, 2003, **425**, 487-490.
3. R. R. Arvizo, S. Bhattacharyya, R. A. Kudgus, K. Giri, R. Bhattacharya and P. Mukherjee, *Chem. Soc. Rev.*, 2012, **41**, 2943-2970.
4. Y. Lu, J. Yuan, F. Polzer, M. Drechsler and J. Preussner, *ACS Nano*, 2010, **4**, 7078-7086.
5. H. Xu, J. Xu, Z. Zhu, H. Liu and S. Liu, *Macromolecules*, 2006, **39**, 8451-8455.
6. P. Zhang, C. Shao, Z. Zhang, M. Zhang, J. Mu, Z. Guo and Y. Liu, *Nanoscale*, 2011, **3**, 3357-3363.
7. S. Saha, A. Pal, S. Kundu, S. Basu and T. Pal, *Langmuir*, 2009, **26**, 2885-2893.
8. Z. Qu, W. Huang, M. Cheng and X. Bao, *J. Phys. Chem. B*, 2005, **109**, 15842-15848.
9. A. de Oliveira, A. Wolf and F. Schüth, *Cataly. Lett.*, 2001, **73**, 157-160.
10. K. Esumi, R. Isono and T. Yoshimura, *Langmuir*, 2004, **20**, 237-243.
11. J. Z. Du and R. K. O'Reilly, *Soft Matter*, 2009, **5**, 3544.
12. W. Z. Yuan, J. R. Wei, H. Lu, L. Fan and J. Z. Du, *Chem. Commun.*, 2012, **48**, 6857-6859.
13. C. Zhang, Y. Q. Zhu, C. C. Zhou, W. Z. Yuan and J. Z. Du, *Polym. Chem.*, 2013, **4**, 255-259.
14. T. B. Ren, Q. M. Liu, H. Lu, H. M. Liu, X. Zhang and J. Z. Du, *J. Mater. Chem.*, 2012, **22**, 12329-12338.
15. A. Lu, P. Cotanda, J. P. Patterson, D. A. Longbottom and R. K. O'Reilly, *Chem. Commun.*, 2012, **48**, 9699-9701.
16. X. Chen, G. Zou, Y. Deng and Q. Zhang, *Nanotechnology*, 2008, **19**.
17. C. V. Rode, M. J. Vaidya and R. V. Chaudhari, *Org. Process. Res. Dev.*, 1999, **3**, 465-470.
18. K. Hayakawa, T. Yoshimura and K. Esumi, *Langmuir*, 2003, **19**, 5517-5521.
19. S. Biella, F. Porta, L. Prati and M. Rossi, *Cataly. Lett.*, 2003, **90**, 23-29.
20. M. M. Mohamed and M. S. Al-Sharif, *Mater. Chem. Phys.*, 2012, **136**, 528-537.
21. K. D. Zou, Q. M. Liu, J. Chen and J. Z. Du, *Polym. Chem.*, 2014, **5**, 405-411.
22. H. Lu, L. Yu, Q. M. Liu and J. Z. Du, *Polym. Chem.*, 2013, **4**, 3448-3452.
23. H. Lu, L. Fan, Q. M. Liu, J. R. Wei, T. B. Ren and J. Z. Du, *Polym. Chem.*, 2012, **3**, 2217-2227.
24. P. Herves, M. Perez-Lorenzo, L. M. Liz-Marzan, J. Dzubiella, Y. Lu and M. Ballauff, *Chem. Soc. Rev.*, 2012, **41**, 5577-5587.
25. H. Song, R. M. Rioux, J. D. Hoefelmeyer, R. Komor, K. Niesz, M. Grass, P. Yang and G. A. Somorjai, *J. Am. Chem. Soc.*, 2006, **128**, 3027-3037.
26. S. Panigrahi, S. Basu, S. Praharaj, S. Pande, S. Jana, A. Pal, S. K. Ghosh and T. Pal, *J. Phys. Chem. C*, 2007, **111**, 4596-4605.
27. S. Wunder, F. Polzer, Y. Lu, Y. Mei and M. Ballauff, *J. Phys. Chem. C*, 2010, **114**, 8814-8820.